Nuclear Instruments and Methods in Physics Research B 541 (2023) 355–362

Contents lists available at ScienceDirect

Nuclear Inst. and Methods in Physics Research, B

journal homepage: www.elsevier.com/locate/nimb

Comparison of the effects of continuous and intermittent electron irradiation on commercial 4H-SiC Schottky barrier diodes

Yisong Wang [a], Meiju Xiang [a], Yao Ma [a,b,*], Min Gong [a,b], Rui Guo [c], Mu He [a], Xuhao Zhu [a], Fan Mei [a], Yun Li [a], Mingmin Huang [a,b], Zhimei Yang [a,b], Jianer Li [d], Zhongbo Hu [d]

[a] Key Laboratory for Microelectronics, College of Physics, Sichuan University, Chengdu 610064, China
[b] Laboratory of Radiation Physics and Technology of Ministry of Education, Sichuan University, Chengdu 610064, China
[c] School of Electronic Science & Engineering, Southeast University, Nanjing 211189, Nanjing, China
[d] Ritam Microelectronic(Sichuan)CO., LTD, Suining 629200, China

ARTICLE INFO

Keywords:
Electron radiation
Continuous
Intermittent
Schottky barrier diodes
Silicon carbide (SiC)

ABSTRACT

The radiation hardness of commercial 4H-SiC Schottky barrier diodes (STPSC1006D) has been investigated in this study. Primarily, intermittent irradiation at 0.5 Hz and continuous irradiation were analyzed and compared. Current–voltage (*I–V*), capacitance–voltage transform deep-level transient spectroscopy (FT-DLTS) were used to characterize the devices before and after irradiation. The devices show stability in their *I–V* characteristics upon irradiation. The free carrier concentration of the devices obtained from the *C–V* results decreased with the increasing of electron fluence. Additionally, new defects were observed after irradiation, which was the reason for the degradation in the electrical properties of the devices. The comparison of the devices irradiated intermittently and those irradiated continuous reveals that intermittent irradiation causes greater changes in electrical properties than continuous irradiation. These characteristics show the impact of STPSC1006D in space applications.

1. Introduction

Silicon carbide (SiC) devices have become attractive for power applications both in space and on Earth. Compared to silicon, SiC is superior for power devices for its higher breakdown field and better thermal conductivity. SiC is a robust material and therefore has the potential to replace Si as the material of choice for high-reliabilityy avionic applications, as it far exceeds the performance of Si in cosmic ray environments, facilitating significant advances in the electrification of aircraft to be made in the near future [1].

There is great interest in studying the response of SiC Schottky barrier diodes (SBDs) to high energy particle radiation because of their potential applications in space, the nuclear power industry, and the military. Many researchers have reported that high energy particles, such as protons [2,3], neutrons [2], electrons [2–7], alpha-particles [2,3], and ion radiation [4,5] can create vacancies, interstitials, and their associated defects [6]. These radiation-induced defects may be coupled with the dopants electrically [2] or act as generation-recombination centers [9,10] in SiC. In the past, researchers primarily focused on the effects of radiation on simple metal/SiC structures such as Ni/SiC and Ti/SiC structures. With the development of the SiC device fabrication process, it is necessary to study the irradiation effects on commercial SiC devices fabricated with complicated structures for application in harsh environments as modern electronic components are known to be very sensitive to the radiative space environment. The presence of high-energy and ion particles such as protons, heavy ions, and electrons induces many observable effects ranging from degradation of performance to functional disruptions that can affect system operations. Satellites may then experience shortened lifetimes or major failures. Also, there are various types of irradiation, each of a different energy range such as trapped electrons in the range of 10 s of MeV [4,5], heavy ions of 100 s of MeV [5], high frequency galactic cosmic rays of GeV [7], high frequency solar energetic particles [8], etc. which affects the electronic components differently and in varying degrees of degradation, like TID (Total Ionizing Dose), or SEE (Single Event Effect) [11], etc. Despite the protection of the earth's magnetic field, electronic devices are still exposed to cosmic radiation of various frequencies on earth, such as solar winds, which affects the electrical properties of the

* Corresponding author.
E-mail address: mayao@scu.edu.cn (Y. Ma).

https://doi.org/10.1016/j.nimb.2023.05.071
Received 23 October 2022; Received in revised form 16 May 2023; Accepted 24 May 2023
Available online 2 June 2023
0168-583X/© 2023 Elsevier B.V. All rights reserved.

devices and even cause failure. Therefore, it is crucial to study the electrical properties of devices under different irradiation frequencies. Installations at high altitudes are much more prone to cosmic ray failures because of the increased irradiation frequency and the total amount of cosmic rays. The exponential dependence of the cosmic ray failure rate on the reverse bias voltage will markedly increase the number of cosmic ray failures when increasing the DC-link voltage [12].

In this study, the behavior of commercial 4H-SiC SBD (STPSC1006D) before and after electron irradiation at different fluences for intermittent and continuous irradiation was investigated. Current–voltage (*I–V*), capacitance–voltage (*C–V*), and Fourier transform deep level transient spectroscopy (FT-DLTS) measurements were performed to study the change in characteristics of the devices induced by the irradiation. The cosmic radiation self-sustaining process "streamer" (self-burning while under irradiation) is known to produce an expansion of the plasma area which eventually causes the drain and source to short-circuit, producing heat that melts the Si and subsequently destroys the MOSFET structure, resulting in device failure [13].

2. Experiment

The devices used in this study were commercial SiC SBDs manufactured by STMicroelectronics: STPSC1006D (600 V, 10 A). Fig. 1 is the figure of the device stack.

The active area for these diodes was measured at 2.3 mm^2. The package materials were removed from the device prior to the irradiation tests to enable the electrons to irradiate the sensitive layers in the device directly, i.e., the Schottky junction and the epitaxial layer. And from the STEM image in Fig. 2, it can be seen that the width of the device is about 3.23 mm. The thickness of the upper electrode is about 1 μm. The metal layer is composed of Ni Sn Pb from bottom to top. In the middle the intermediate silicon carbide and its epitaxial layer thickness is 225 μm. The thickness of the lower electrode is about 1.3 μm. The type of its metal is similar to that of the upper electrode.

The devices were irradiated with 1.7 MeV electrons produced in the electron beam accelerator at Sichuan Institute of Atomic Energy (SIAE) in Chengdu, China. All the irradiations and device characterizations were done at room temperature, and the electron beams were at normal incidence to the device surface. The electron flux was 1×10^{14} e/cm^2·s and the independent fluences were 1×10^{14} e/cm^2, 1×10^{15} e/cm^2, and 1×10^{16} e/cm^2. In addition, all electrodes of the diodes were floated during irradiation, and the intermittent radiation frequency was 0.5 Hz. The 4H-SiC samples were irradiated by a 1.7 MeV electron beam using the GJ-2 SIAE high-frequency high-voltage electron accelerator. A series of samples were irradiated in two groups. The cars interchanged with the samples have the same speed and different travel distances, which determines the cooling time for each group, and the total effect can be calculated due to the speed and duration of the cars. The car reciprocates with the sample and has the same speed and different moving distance that decides the cooling time of each group and the total influence can be calculated due to the speed of the car and time of duration. Group (1) was irradiated by a continuous beam (which had a small interval between irradiation), while group (2) was irradiated by an intermittent beam so it had a greater cooling time.

Agilent B1500A and B2902A semiconductor parameter analyzers were used to measure the *C–V* and *I–V* characteristics. Thereafter, the device was placed in a closed-cycle helium cryostat and characterized by FT1230 FT-DLTS in a wide temperature range. All of these measurements were performed on the devices both before irradiation as well as after. The sample is stored in liquid nitrogen after irradiation, and all tests are completed within 24 h. The following are the experimental parameters.

3. Results and discussion

3.1. C–V characteristics

The C^{-2} (pF^{-2}) as a function of the reverse bias voltage, V_R (V), before and after irradiation measured from − 20 V to 0 V at 1 MHz is shown in Fig. 3.

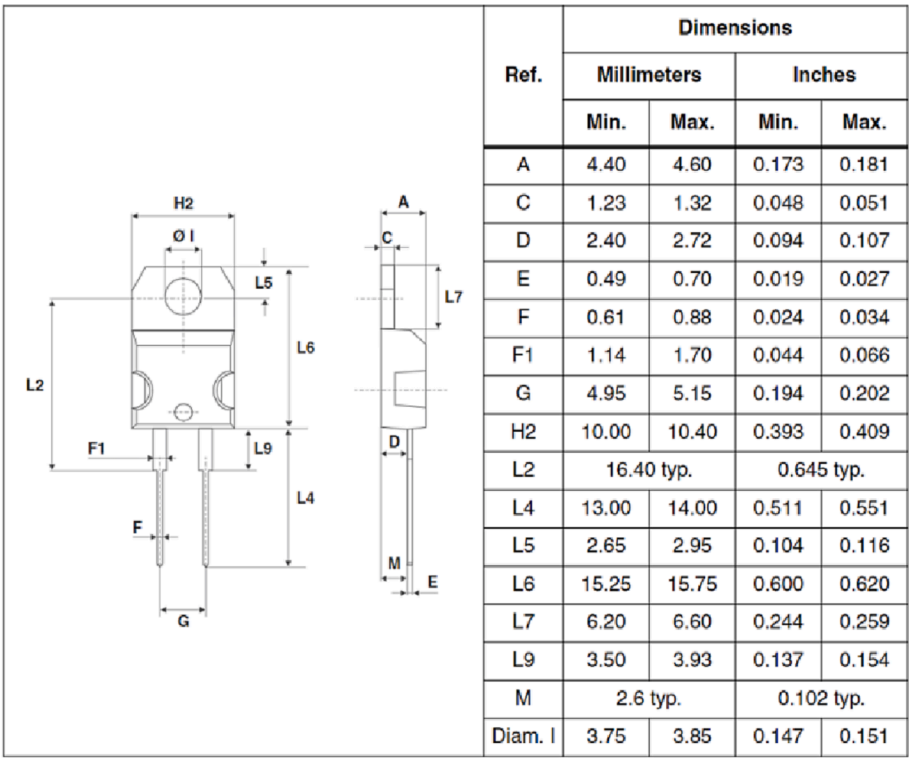

Ref.	Dimensions			
	Millimeters		Inches	
	Min.	Max.	Min.	Max.
A	4.40	4.60	0.173	0.181
C	1.23	1.32	0.048	0.051
D	2.40	2.72	0.094	0.107
E	0.49	0.70	0.019	0.027
F	0.61	0.88	0.024	0.034
F1	1.14	1.70	0.044	0.066
G	4.95	5.15	0.194	0.202
H2	10.00	10.40	0.393	0.409
L2	16.40 typ.		0.645 typ.	
L4	13.00	14.00	0.511	0.551
L5	2.65	2.95	0.104	0.116
L6	15.25	15.75	0.600	0.620
L7	6.20	6.60	0.244	0.259
L9	3.50	3.93	0.137	0.154
M	2.6 typ.		0.102 typ.	
Diam. I	3.75	3.85	0.147	0.151

Fig. 1. Schematic diagram of STPSC1006D.

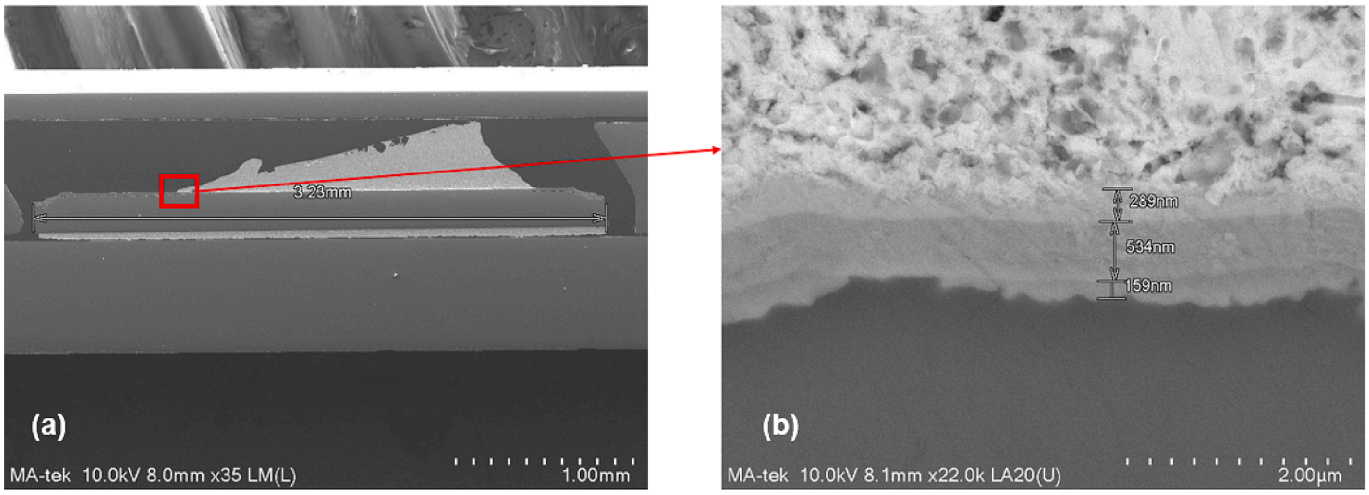

Fig. 2. (a) The STEM image of STPSC1006D (b) Partial zoomed-in image.

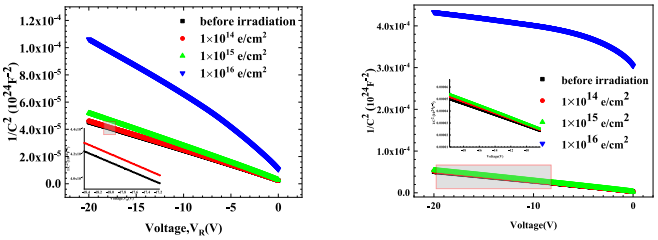

Fig. 3. C^{-2}–V characteristics of Schottky barrier diodes of n-4H-SiC (STPSC1006D) before and after: (a) continuous electron irradiation; (b) intermittent electron irradiation.

The C–V characteristics changed more significantly with increasing electron fluences. The slope of the C^{-2}–V_R is approximately constant for all diodes, which indicates that all of the dopants were ionized due to the presence of the electric field [14,15]. The effective free carrier concentration (N_{net}), built-in potential (V_{bi}), and Schottky barrier height ($q\phi_{C\text{-}V}$) were determined from the plot and tabulated in Tables 1 and 2. The N_{net}, decreased with irradiation because of the defects introduced by the electron irradiation into the SiC.

$$\frac{1}{C^2} = \frac{2(V_{bi} - V_R)}{q\varepsilon_s\varepsilon_0 A^2 N_{net}}; \tag{1}$$

where q is the charge, ε_s is the semiconductor permittivity, ε_0 is the permittivity of free space, A is the effective area of the diode, and V_{bi} is obtained from the intercept of reverse voltage when C^{-2} is equal to zero. The zero-bias barrier heights for both devices were determined from Eq.

Table 1
Experimental parameters.

Radiation fluence (e/cm^2)	Test mode	Irradiation mode
1×10^{14}	Forward current test Reverse current test Reverse capacitance test	continuous irradiation intermittent irradiation
1×10^{15}	Deep level transient spectrum test	continuous irradiation intermittent irradiation
1×10^{16}		continuous irradiation intermittent irradiation

Table 2
Electrical performance parameters of the SiC SBD.

Continuous irradiation			Intermittent irradiation		
fluence (e/cm^2)	N_{net} (cm^{-3})	$q\phi_{C\text{-}V}$ (eV)	fluence (e/cm^2)	N_{net} (cm^{-3})	$q\phi_{C\text{-}V}$ (eV)
0	1.29×10^{16}	1.34	0	1.03×10^{16}	1.42
1×10^{14}	1.27×10^{16}	1.35	1×10^{14}	1.08×10^{16}	1.45
1×10^{15}	1.13×10^{16}	1.44	1×10^{15}	1.01×10^{16}	1.47
1×10^{16}	6.44×10^{15}	2.15	1×10^{16}	2.20×10^{15}	26.05

(2):

$$\phi_{C-V} = V_{bi} + \frac{kT}{q} ln \frac{N_c}{N_{net}} + \frac{kT}{q}; \tag{2}$$

where k is the Boltzmann constant, T is the absolute temperature in K, and N_c is the effective density of states in the conduction band. The extracted parameters are shown in the following table. The plot in Fig. 3 (a) and (b) was deduced from Eq. (1), which represents the depletion layer in Schottky diodes.

From Fig. 1, the N_{net} of the device was determined from the slope of the plots according to Eq. (1). The free carrier removal rate, η, can be obtained from Eq. (3), below:

$$\eta = \frac{\Delta(N_D - N_A)}{\varphi}; \tag{3}$$

where $\Delta(N_D - N_A)$ is the change in N_{net} before and after irradiation and φ is the fluence at which the device was bombarded [16]. At room temperature (300 K), the change with a fluence of 1×10^{14} e/cm^2, 1×10^{15} e/cm^2, and 1×10^{16} e/cm^2 in N_{net} was from 1.29×10^{16} cm^{-3} to 1.27×10^{16} cm^{-3}, 1.13×10^{16} cm^{-3}, and 6.44×10^{15} cm^{-3}, and the η was calculated as 2.00 cm^{-1}, 0.80 cm^{-1}, and 0.65 cm^{-1}. It is clear that the η decreased with increasing electron fluence. Furthermore, the findings agree with the η of 1.67 cm^{-1} for the electron fluence of 6×10^{14} e/cm^2 reported by E. Omotoso et al. [6,7].

The decrease of N_{net} in SiC after electron irradiation is due to the defects introduced by the irradiation. Some defects act as trap centers to capture free carriers, and the Si vacancies and impurity interstitial atoms caused by irradiation deactivate the doped impurities. The combined effect of these two radiation damages decreases the effective current-carrying in SiC concentration. From Table 3 we can get that

Table 3
Electrical performance parameters of SiC SBD under continuous irradiation group.

Fluence (e/cm^2)	V_{on}(V)	n	SBH_{I-V} (eV)	R_s (Ω)	N_{net} (cm^{-3})	V_{bi} (V)	SBH_{C-V} (eV)
0	0.70	1.05	1.11	0.63	1.19×10^{16}	1.11	1.34
1×10^{14}	0.69	1.07	1.14	0.64	1.19×10^{16}	1.11	1.35
1×10^{15}	0.69	1.08	1.13	0.68	1.06×10^{16}	1.20	1.44
1×10^{16}	0.71	1.12	1.12	0.83	4.41×10^{15}	1.91	2.15

comparing the N_{net} of the two types of irradiations under the maximum irradiation fluence of 1×10^{16} e/cm^2 before and after irradiation, a significant reduction in N_{net} was observed after irradiation in both sets of devices. Compared with continuous irradiation, intermittent irradiation has less effect on temperature rise, and annealing is not obvious enough, so N_{net} increases. In addition, from the theoretical capacitance–voltage formula of SBD, if the effective doping concentration distribution of the epitaxial layer is uniform, the fitting curve C^{-2}–V obtained from the C–V characteristic should theoretically be a straight line, with its slope being the effective load. As a function of carrier concentration N_{net}, the higher the N_{net} of the substrate, the lower the absolute value of the slope of the fitted curve C^{-2}–V.

The fitted curves under both continuous and intermittent irradiation have better linearity at the two lower irradiation fluences, and the absolute value of the slope increases with the increase of the irradiation fluence. According to the C^{-2}–V relation in SBD, the absolute value of the slope of the fitted curve is inversely proportional to the N_{net} of the semiconductor, meaning, the N_{net} decreases with the increase in irradiation fluence, indicating that the longitudinal distribution of the carrier concentration in the epitaxial layer of the device before irradiation was uniform. Table 4 shows that the N_{net} of the continuous irradiated and intermittently irradiated devices before irradiation were 1.29×10^{16} cm^{-2} and 1.03×10^{16} cm^{-2}, respectively and increases with the decrease in irradiation fluence. At or below the irradiation fluence of 1×10^{15} e/cm^2, the N_{net} of the device in the vertical direction remained evenly distributed. When the irradiation fluence reached 1×10^{16} e/cm^2, however, the linearity of the C^{-2}–V curve in the test range changed, indicating that the N_{net} became unevenly distributed with depth. Thus, the N_{net} at the intermittent group interface is lower than the N_{net} far away from the interface. As far as the N_{net} is concerned, the radiation damage caused by the SiC near the upper interface is higher than the radiation damage of the SiC far away from the interface. Based on the semiconductor conductivity formula, this is because the defects introduced by the radiation affect the scattering mechanism of the carriers, changing the mobility of the carriers. Moreover, the high temperature annealing effect accompanying continuous irradiation causes the effects on the devices to be different from those under intermittent irradiation.

Table 4
Electrical performance parameters of SiC SBD in intermittent irradiation group.

Fluence (e/cm^2)	V_{on}(V)	n	SBH_{I-V} (eV)	R_s (Ω)	N_{net} (cm^{-3})	V_{bi} (V)	SBH_{C-V} (eV)
0	0.69	1.04	1.20	0.49	1.03×10^{16}	1.18	1.42
1×10^{14}	0.71	1.04	1.20	0.50	1.08×10^{16}	1.22	1.45
1×10^{15}	0.71	1.04	1.20	0.51	1.01×10^{16}	1.24	1.47
1×10^{16}	0.81	1.57	1.01	12.64	2.20×10^{15}	25.77	26.05

3.2. I–V characteristics

Fig. 3 shows the forward bias characteristics of the STPSC1006D diodes from 0 V to 3.5 V before and after irradiation. It shows that the forward current decreased with increasing electron fluence. After continuous electron irradiation with a fluence of 1×10^{14} e/cm^2, 1×10^{15} e/cm^2, and 1×10^{16} e/cm^2, the current due to forward bias of 2 V decreased from 0.74 A to 0.73 A, 0.71 A, and 0.56 A, corresponding to intermittent group respectively, i.e., a 24% reduction in forward current was induced by the electron irradiation at the highest fluence of 1×10^{16} e/cm^2. The effect of irradiation on the STPSC1006D diodes can be quantified in terms of the ideality factor (n), Schottky barrier height (ϕ_{I-V}), and series resistance (R_S) obtained from the I–V plots. Measurements on the Schottky contacts were taken both before and after the devices were irradiated. The ϕ_{I-V} of the contacts were determined from the I–V characteristics analyzed using the thermionic emission model, based on which the forward current (I_F) through the SiC SBD can be expressed as [13]:

$$I_F = I_S\left\{\exp\left[\frac{q}{nkT}(V - I_F R_S)\right] - 1\right\}; \quad (4)$$

$$I_S = AA^*T^2\exp(-q\phi_{I-V}/kT); \quad (5)$$

where, A^* is Richardson's constant (146 $A{\cdot}cm^{-2}{\cdot}K^{-2}$).

Fig. 4(a) and (b) show the forward bias characteristics of the SiC SBD device under different irradiation fluences after continuous and intermittent electron irradiation, respectively. The forward bias characteristics are important in understanding the forward bias conduction characteristics and extracting important electrical parameters, such as the n, ϕ_{I-V}, and R_S of the SBD.

From Fig. 4, after electron irradiation, notable decrease in the forward bias current of the SiC SBDs is observed, and both irradiation methods exhibit similar trends with regards to the electron irradiation fluence. For the fluences of 1×10^{14} e/cm^2 and 1×10^{15} e/cm^2, the forward bias current only reduces slightly. At the fluence of 1×10^{16} e/cm^2, however, the forward bias current of the SBDs under both types of irradiation decreases significantly. The forward voltage at 2 V under continuous irradiation decreases from 0.73A at 1×10^{14} e/cm^2 to 0.71A at 1×10^{15} e/cm^2 and 0.68A at 1×10^{16} e/cm^2 with the increase of irradiation fluence, which have decreased by about 3.2% and 5.1% respectively. Although the forward bias characteristics of the device under both types of irradiation show similar trends with the irradiation fluence, greater degradation was observed under intermittent irradiation, especially at 1×10^{16} e/cm^2, where the current drops by 92% (2.18 A to 0.18 A) corresponding to a forward bias voltage of 2 V. Thus, intermittent irradiation results in greater degradation in the forward bias characteristics of the device.

Fig. 5(a) and (b) are the reverse bias I–V characteristics under continuous and intermittent irradiation, respectively, for the aforementioned three different electron irradiation fluences. Herein, the reverse bias current of the device does not change significantly after continuous electron irradiation. Under intermittent irradiation, however, the reverse bias current increases. This is due to the defects introduced by the irradiation, which decrease the Schottky barrier height (SBH) of the SBD and increase the number of the recombination centers. The reduction of the SBH increases the thermionic emission current (I_0) and tunneling current (I_T), and the increase in the recombination centers reduces the carrier lifetime, which in turn increases the recombination current (I_W). Fig. 5 also shows that the SBH of the device under the fluence of 1×10^{14} e/cm^2 is the same as that before irradiation, and its reverse bias current is the smallest, indicating that the recombination centers generated by irradiation at this fluence is the main reason for the increase in current.

Using the parameter extraction method, the R_S is extracted from the forward bias I–V characteristics of the device, which is similar to the change of ideality factor and Schottky barrier with irradiation. The R_S

A^* is Richardson's constant (146 A·cm^{-2}·K^{-2}).

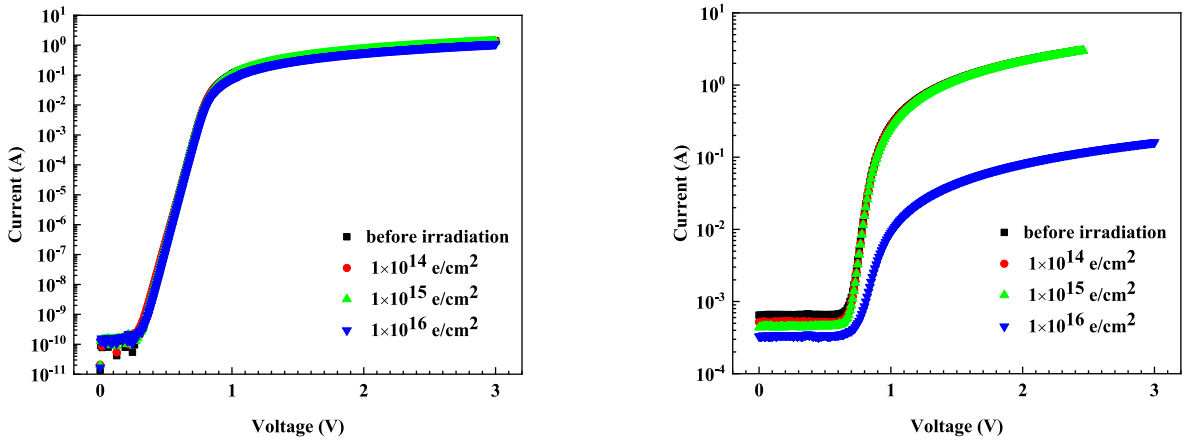

Fig. 4. Forward bias *I–V* characteristics of SiC SBD under: (a) continuous irradiation; (b) intermittent irradiation of different electron irradiation fluences.

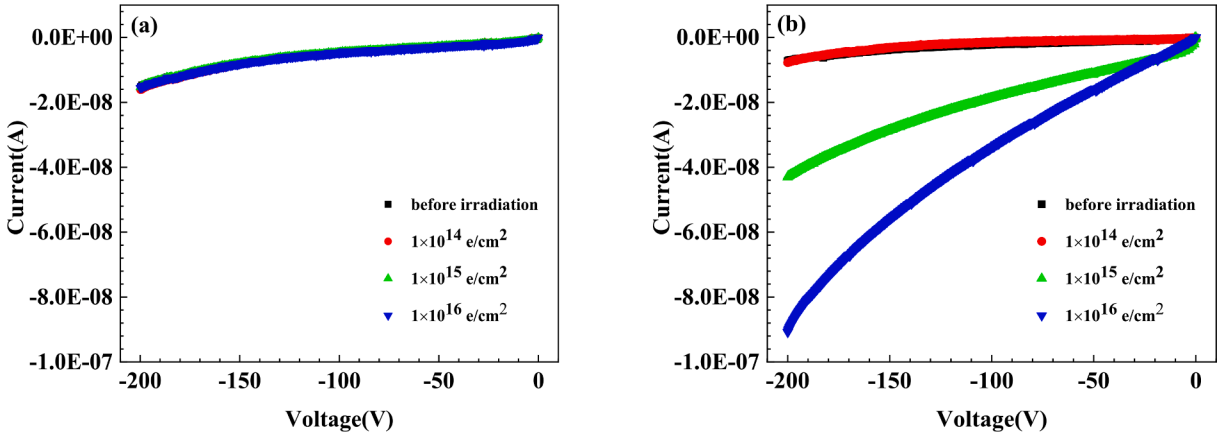

Fig. 5. Reverse bias *I–V* curves of SiC SBD under: (a) continuous irradiation; (b) intermittent irradiation (b) for different electron irradiation fluences.

under either type of irradiation did not change significantly at fluences of 1 × 10^{14} e/cm^2 and 1 × 10^{15} e/cm^2, indicating that the device has good radiation stability as long the fluence is kept at around or less than 1 × 10^{15} e/cm^2. However, at the fluence of 1 × 10^{16} e/cm^2, the SiC SBD R_S increased significantly from 0.49 Ω before irradiation to 12.64 Ω after. This is possibly due to the creation of carrier trap centers in the SiC and impurity deactivation effects. Due to the trap centers and the scattering effects of radiation-generated defects, the effective carrier concentration and mobility of the substrate are reduced, resulting in a decrease in the conductivity of the device, i.e, an increase in the R_S; and higher fluences of radiation create greater numbers of defects in the SiC, enhancing the trapping and scattering of carriers, and greatly increasing the R_S. Additionally, a significant difference was observed in the increase of the R_S of the devices between the two irradiation types. Upon the fluence of 1 × 10^{16} e/cm2, the R_S after continuous irradiation increases from 0.63 Ω before irradiation to 0.84 Ω after, while the R_S after intermittent irradiation increased from 0.49 Ω before irradiation to 12.64 Ω after as been mentioned earlier. This difference is because of the annealing effect of the continuous irradiation process due to which the lattice of the SiC substrate is lattice repaired and the impurities are reactivated. Therefore, the activation of doped impurities at the high temperatures developed increases the N_{net}, and the decrease of the defect concentration also weakens the carrier scattering effect, restoring carrier mobility. The N_{net} and mobility are restored. Hence, only a slight increase in R_S is observed under continuous irradiation despite the exposure to high fluences. During the irradiation process, electrons transfer energy to the lattice through collisions with the lattice; thus, continuous irradiation causes the device temperature to continuous to rise, resulting in a high-temperature annealing effect, which in turn reduces the recombination centers introduced by the electron irradiation in the SiC. Under high frequency irradiation, the Schottky barrier and the opening voltage increase significantly due to the enhancement of the storage effect of minority carriers and the transit time effect in the insulation layer. The irradiation flux is about 70 W/m^2. According to Newton's cooling law, the higher the temperature, the faster the object dissipates heat, and the heat obtained from the radiation flux is a constant value, so there is an extreme value for the temperature of the sample. According to the worst estimate of the material characteristics and heat dissipation of the irradiated device, the temperature gradually remains constant when the sample temperature is about 500 K, while the irradiation time required for the three doses in the experiment increases exponentially, so the temperature extremes will obviously be reached under continuous irradiation.

The increase of the *n* indicates that after electron irradiation, the current transport mechanism dominated by thermionic emission in SiC SBD had changed. This is due to the introduction of recombination centers in the SiC substrate by irradiation, which increases the forward bias current. Under intermittent irradiation, the *n* did not change under

low irradiation fluences, indicating that the current mechanism was not affected, which means the main current is still the diffusion current. However, at the fluence of 1×10^{16} e/cm^2, the n of the SBD under intermittent irradiation increased from 1.04 to 1.57, an increase of 0.53 compared with the increase of 0.07 under continuous irradiation. This shows that under the high electron irradiation fluences, intermittent irradiation also introduces recombination centers in the SiC like under continuous irradiation, which increases the recombination rate of minority carriers and reduces carrier lifetime, so the I_W increases, changing the SiC SBD current-carrying mechanism. The reason the increase in n caused by intermittent irradiation was significantly higher than that by continuous irradiation is the weaker annealing effect of the former compared with the latter. However, in intermittent irradiation, the device is intermittently bombarded with the electron as opposed to continuously, resulting in cooling during the lapses in radiation, and therefore, a weaker annealing effect.

3.3. Deep level transient spectroscopy

A DLTS test was performed using an FT-DLTS system before and after ~~the~~ continuous and intermittent electron irradiation. Fig. 6 shows the FT-DLTS spectra performed in the temperature range 20–450 K, at a quiescent reverse bias of − 5.0 V, filling pulse amplitude of 5.0 V, filling pulse width of 100 μs, period width of 192 ms, and related rate window of 12 s^{-1} for continuous irradiation. According to Fig. 6, no peak was observed in the test temperature range before the irradiation, and a peak located at 289 K with a shoulder was observed after irradiation at the fluence of 1×10^{14} e/cm^2. Fig. 7 shows the Arrhenius plot of ln(e_n(T)/T^2) where $e_n(T) = AT^2\exp(-\frac{E}{KT})$ [17–19] versus 1000/T of the related defect. The extracted parameters obtain defect data as shown in Table 5 (Including the following intermittent irradiation group). The signatures of the defect in terms of activation energies (E_n) and apparent capture cross sections (σ_n) determined from Fig. 7 were 0.644 eV and 3.26×10^{15} cm^{-2}, respectively, according to the method earlier reported by [4]. This defect has been designated in the literature as $Z_{1/2}$ [2,3]. With the increase in electron fluence, the peak becomes significantly higher and broader. This suggests that the density of the defects increases, and other defects such as silicon vacancies (v_{Si}) and carbon vacancies (v_C) earlier reported in [9,20] were induced in the SiC with increasing fluence. For intermittent irradiation, by a large error in the E_N, however, these levels can be seen together in some spectra, which shows that these

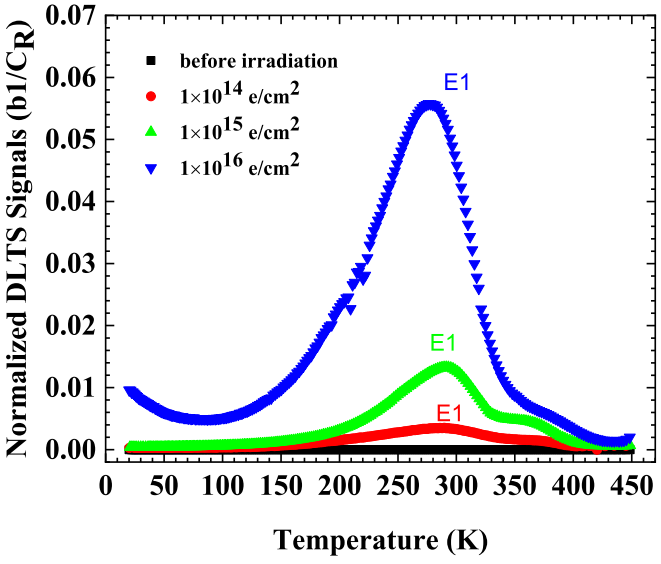

Fig. 6. DLTS spectra of STPSC106D SiC SBDs before and after 1.7 MeV continuous continuous electron irradiation with different electron fluences of 1 × 10^{14}, 1 × 10^{15}, and 1 × 10^{16} e/cm^2.

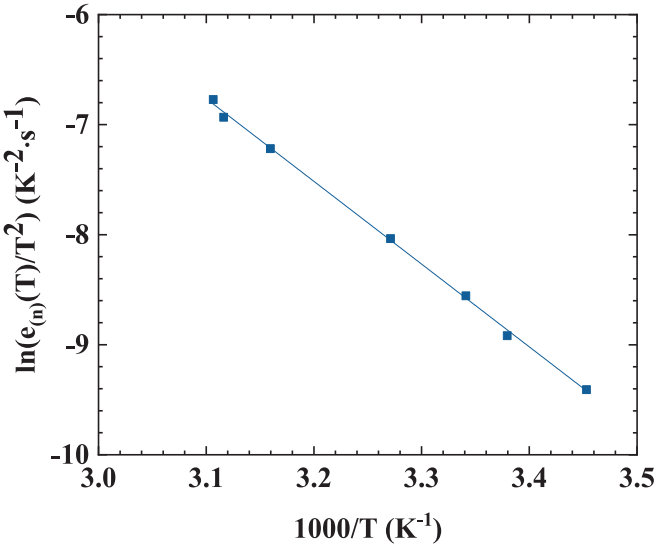

Fig. 7. Arrhenius plot of the observed peak at 298 K after 1.5 7 MeV continuous electron irradiation.

Table 5
Characteristic values of deep level defects for devices irradiated by 1.7 MeV electron irradiation.

Irradiation fluence (e/cm^2)	Peak position	Energy Level Position E_C-E_T (eV)	capture cross section σ_n (cm^2)	Identity and Charge states
continuous electron irradiation				
1×10^{14}/1×10^{15}/1×10^{16}	E1	0.64	3.26×10^{-15}	$Z_{1/2}$
intermittent electron irradiation				
1×10^{14}	E1	0.68	5.49×10^{-15}	$Z_{1/2}$
1×10^{15}	E2	0.71	2.48×10^{-15}	$Z_{1/2}$
	E3	1.12	6.71×10^{-17}	EH_5
1×10^{16}	E4	0.72	5.17×10^{-15}	$Z_{1/2}$
	E5	1.09	1.44×10^{-17}	EH_5
	E6	0.16	4.01×10^{-15}	Ti(h)

peaks belong to different defects as one transition cannot be attributed to different levels [21–23] (Fig. 8).

The DLTS spectra for intermittent irradiation are shown in Fig. 9. Here, the $Z_{1/2}$ center has been established as the major lifetime killing defect in 4H-SiC and identified as either v_{Si} or v_C as discussed above. With increasing irradiation fluence, more defects appear in the devices. The peak E2 and E4 appeared in the device at the fluence of 1×10^{15} e/cm^2 and 1×10^{16} e/cm^2. This level has been attributed to the EH5 trap center. Ti impurity lodged in a cubic Si lattice site has been attributed to E6 in 1×10^{16} e/cm^2. The presence of irradiation-induced deep levels alters the charge balance in the material and, through Fermi–Dirac statistics, changes the position of the Fermi level, thereby affecting the N_{net}. The type of defects due to intermittent irradiation increased with intermittent electron irradiation, which means ~~while~~ that during the irradiation interval, the cooling process of intermittent irradiation, the device temperature can be kept at a lower temperature to complete the irradiation experiment of the target fluence so that the annealing effect during the irradiation process is weaker than that of the irradiation group. The impurity vacancy (Ti & EH5) deeper than the carbon vacancy ($Z_{1/2}$) is generated, so greater forward and reverse current changes are generated for intermittent irradiation with the same total fluence

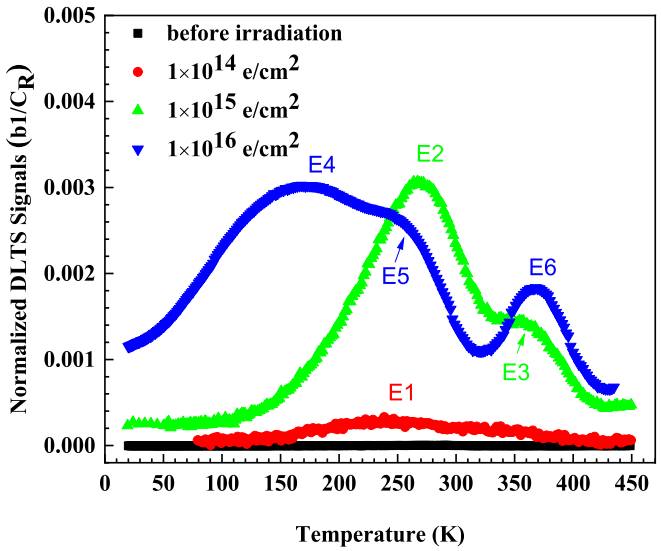

Fig. 8. DLTS spectra of STPSC106D SiC SBDs before and after 1.7 MeV intermittent electron irradiation with different electron fluences of 1×10^{14} (amplified × 20), 1×10^{15} (amplified × 2), and 1×10^{16} e/cm^2.

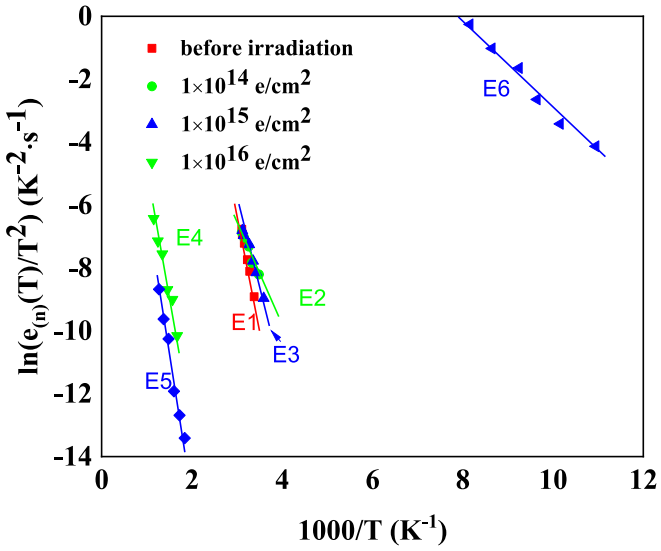

Fig. 9. Arrhenius plot of the observed peak at 298 K after 1.7 MeV intermittent electron irradiation.

[24–28].

4. Conclusions

It is of much importance to study the electrical properties of devices under different irradiation frequencies rates. In this study, continuous and intermittent electron irradiation of 1.7 MeV upon commercial 4H-SiC SBDs (STPSC1006D) were investigated. From the *I–V* measurements, upon irradiation, although the characteristic parameters changed slightly, the current transport mechanism was still dominated by thermionic emission at room temperature. In addition, there was no significant change in the reverse bias current after irradiation, which means that the diodes retained good rectification characteristics after the irradiation. Under high frequency irradiation, the Schottky barrier and the opening voltage increase significantly due to the enhancement of the storage effect of minority carriers and the transit time effect in the insulation layer. The *C–V* measurements revealed a decrease in the free carrier concentration with increasing electron fluence. The effects of electron irradiation on STPSC1006D diodes were also investigated using high-energy-resolution FT-DLTS measured in a wide temperature range of 20–450 K. The experimental results revealed that the diodes have good defect control, and the bulk defect named $Z_{1/2}$, EH5, Ti center acted as generation and combination centers after irradiation. The decrease in free carrier concentration after the irradiation may be attributed to other defects that not separated from the broad DLTS peak. Therefore, it is understood that the electrical characteristics were influenced by the induced deep level centers induced by electron irradiation. All results show that although the device performance was effected by electron irradiation with all electrodes floated, the diodes still operate normally at fluences about and below 1×10^{15} e/cm^2; but the performance of the device had degraded significantly after irradiation at higher fluences. Installations at high altitude are much more prone to cosmic ray failures because of the increased irradiation frequency and the total amount of cosmic ray. The exponential dependence of the cosmic ray failure rate on the reverse bias voltage will markedly increase the amount of cosmic ray failures when increasing the DC-link voltage. In general, the performance degradation due to intermittent irradiation was more severe than that of continuous irradiation, with the more kinds of defects generated as well.

CRediT authorship contribution statement

Yisong Wang: Validation, Writing – original draft. **Meiju Xiang:** Formal analysis. **Yao Ma:** Funding acquisition, Project administration, Supervision, Writing – review & editing. **Min Gong:** Project administration, Resources. **Rui Guo:** Validation. **Mu He:** Visualization. **Yun Li:** Project administration. **Mingmin Huang:** Project administration, Validation. **Zhimei Yang:** Funding acquisition, Writing – review & editing. **Jianer Li:** Data curation.

Declaration of Competing Interest

The authors declare that they have no known competing financial interests or personal relationships that could have appeared to influence the work reported in this paper.

Data availability

Data will be made available on request.

Acknowledgments

This project is supported by the fund of Innovation Center of Radiation Application under Grant No. KFZC2020021001, the Natural Science Foundation of Sichuan Province under Grant No. 2020NSFSC087. We do thank for the contribution of Peichun Zou and Xue Zhao from Sichuan Xu Mao Micro Technology in the work of XTEM test.

References

[1] M.T.M. Littlefair, et al., Single event burnout sensitivity of SiC and Si, Semicond. Sci. Technol. 37 (2022) 065013.
[2] J. Garcia Lopez, M.C. Jimenez-Ramos, M. Rodriguez-Ramos, J. Ceballos, F. Linez, J. Raisanen, Comparative study by IBIC of Si and SiC diodes irradiated with high energy protons, Nucl. Instrum. Methods Phys. Res. Sect. B 372 (2016) 143–150.
[3] S. Nigam, J. Kim, F. Ren, G.Y. Chung, M.F. MacMillan, R. Dwivedi, T.N. Fogarty, R. Wilkins, K.K. Allums, C.R. Abernathy, S.J. Pearton, J.R. Williams, High energy proton irradiation effects on SiC Schottky rectifiers, Appl. Phys. Lett. 81 (13) (2002) 2385–2387.
[4] B. Tsuchiya, T. Shikama, S. Nagata, K. Saito, T. Nozawa, Dynamic measurements of radiation-induced electrical property modifications in CVD-SiC under fast neutron irradiation, J. Nucl. Mater. 455 (1-3) (2014) 645–648.
[5] C. Hemmingsson, N.T. Son, O. Kordina, J.P. Bergman, E. Janzén, J.L. Lindström, S. Savage, N. Nordell, Deep level defects in electron-irradiated 4H SiC epitaxial layers, J. Appl. Phys. 81 (9) (1997) 6155–6159.
[6] E. Omotoso, W.E. Meyer, F.D. Auret, A.T. Paradzah, M. Diale, S.M.M. Coelho, P. J. Janse van Rensburg, P.N.M. Ngoepe, Effects of 5.4 MeV alpha-particle

irradiation on the electrical properties of nickel Schottky diodes on 4H–SiC, Nucl. Instrum. Methods Phys. Res. Sect. B 365 (2015) 264–268.
[7] E. Omotoso, W.E. Meyer, F.D. Auret, et al., Electrical characterization of deep levels created by bombarding nitrogen-doped 4H-SiC with alpha-particle irradiation, Nucl. Instrum. Methods Phys. Res. Sect. B Beam Interact. Mater. Atoms 371 (2016) 312–316.
[8] Ž. Pastuović, I. Capan, D.D. Cohen, J. Forneris, N. Iwamoto, T. Ohshima, R. Siegele, N. Hoshino, H. Tsuchida, Radiation hardness of n-type SiC Schottky barrier diodes irradiated with MeV He ion microbeam, Nucl. Instrum. Methods Phys. Res. Sect. B 348 (2015) 233–239.
[9] Z. Yang, Y. Ma, M. Gong, Y. Li, M. Huang, B.o. Gao, X. Zhao, Recrystallization effects of swift heavy 209 Bi ions irradiation on electrical degradation in 4H-SiC Schottky barrier diode, Nucl. Instrum. Methods Phys. Res. Sect. B 401 (2017) 51–55.
[10] Z. Lin, Z. Yi-Men, Z. Yu-Ming, H. Chao, M.a. Yong-Ji, High energy electron radiation effect on Ni and Ti/4H-SiC Schottky barrier diodes at room temperature, Chin. Phys. B 18 (5) (2009) 1931–1934.
[11] D. Åberg, H. Allen, P. Pellegrino, et al., Nitrogen deactivation by implantation-induced defects in 4H-SiC epitaxial layers, Appl. Phys. Lett. 78 (2001) 2908–2910.
[12] U. Scheuermann, U. Schilling, Impact of device technology on cosmic ray failures in power modules, IET Power Elec. 9 (10) (2016) 2027–2035.
[13] E. Stadnichuk, E. Svechnikova, The criterion for self-sustaining production of relativistic runaway electron avalanches by the positron feedback in thunderstorms, Atmos. Res. 277 (2022) 106329.
[14] S. Ganiyev, N. Muridan, N.F. Hasbullah, Y. Abdullah, Electrical simulation of Ni/4H-SiC Schottky diodes before and after low energy electron radiation, in: 2015 IEEE Regional Symposium on Micro and Nanoelectronics (RSM), Kuala Terengganu, Malaysia, 2015, pp. 1-4, doi: 10.1109/RSM.2015.7354995.
[15] F.D. Auret, S.A. Goodman, M. Hayes, et al., Electrical characterization of 1.8 MeV proton-bombarded ZnO, Appl. Phys. Lett. 79 (2001) 3074–3076.
[16] M. Gong, S. Fung, C.D. Beling, G. Brauer, H. Wirth, W. Skorupa, Gallium implantation induced deep levels in n-type 6H-SIC, J. Appl. Phys. 85 (1) (1999) 105–107.
[17] T. Dalibor, G. Pensl, H. Matsunami, T. Kimoto, W.J. Choyke, A. Schöner, N. Nordell, Deep defect centers in silicon carbide monitored with deep level transient spectroscopy, Phys. Stat. Sol. 162 (1) (1997) 199–225.
[18] I. Pintilie, L. Pintilie, K. Irmscher, B. Thomas, Formation of the Z1,2 deep-level defects in 4H-SiC epitaxial layers: evidence for nitrogen participation, Appl. Phys. Lett. 81 (25) (2002) 4841–4843.
[19] Y. Katoh, L.L. Snead, I. Szlufarska, et al., Radiation effects in SiC for nuclear structural applications, Curr. Opin. Solid State Mater. Sci. 16 (3) (2012) 143–152.
[20] D.V. Lang, Deep-level transient spectroscopy: a new method to characterize traps in semiconductors, J. Appl. Phys. 45 (1974) 3023.
[21] D. Hu, J. Zhang, Y. Jia, Y.u. Wu, L. Peng, Y. Tang, Impact of different gate biases on irradiation and annealing responses of SiC MOSFETs, IEEE Trans. Electron Devices 65 (9) (2018) 3719–3724.
[22] Z. Zhang, Z. Wang, Y. Guo, J. Robertson, Carbon cluster formation and mobility degradation in 4H-SiC MOSFETs, Appl. Phys. Lett. 118 (3) (2021) 031601.
[23] A.C. Ahyi, S. Wang, J. Williams, Gamma irradiation effects on 4H-SiC MOS capacitors and MOSFETs, Mater. Sci. Forum 527–529 (2006) 1063–1066.
[24] J.M. Akturk, A. Mcgarrity, S. Potbhare, et al., Radiation effects in commercial 1200 V 24 A silicon carbide power MOSFETs, IEEE Trans. Nucl. Sci. 59 (6) (2012) 3258–3264.
[25] K. Murata, S. Mitomo, T. Matsuda, T. Yokoseki, T. Makino, S. Onoda, A. Takeyama, T. Ohshima, S. Okubo, Y. Tanaka, M. Kandori, T. Yoshie, Y. Hijikata, Impacts of gate bias and its variation on gamma-ray irradiation resistance of SiC MOSFETs, Phys. Status Solidi 214 (4) (2017) 1600446.
[26] M. Pejović, Processes in radiation sensitive MOSFETs during irradiation and post irradiation annealing responsible for threshold voltage shift, Radiat. Phys. Chem. 130 (2017) 221–228.
[27] D.C. Sheridan, G. Chung, S. Clark, The effects of high-dose gamma irradiation on high-voltage 4H-SiC Schottky diodes and the SiC-SiO2 interface, IEEE Trans. Nucl. Sci. 48 (6) (2001) 2229–2232.
[28] M. Yoshikawa, H. Itoh, Y. Morita, et al., Effects of gamma-ray irradiation on cubic silicon carbide metal-oxide -semiconductor structure, J. Appl. Phys. 70 (3) (1991) 1309–1312.